

---

# Enhancing Pre-Training Data Detection through Distribution Shape Analysis: A Multi-Scale Weighted Residual Approach to Min-K%++

---

Anonymous Author(s)

Affiliation

Address

email

## Abstract

Pre-training data detection in large language models has emerged as a critical challenge for model transparency and compliance, with membership inference attacks serving as the primary mechanism for identifying whether specific text sequences were part of a model's training data. While Min-K%++ represents the current state-of-the-art approach, it suffers from a fundamental limitation: uniform aggregation of token-level scores ignores valuable distributional patterns that could enhance detection accuracy. We propose a novel enhancement through residual score decomposition with multi-scale importance weighting, which analyzes distribution shape features such as skewness, kurtosis, and entropy to reveal training versus non-training patterns. Our method decomposes Min-K%++ scores into trend and residual components using exponential moving averages (Lucas & Sacucci, 1990), applies position-based weighting that emphasizes earlier tokens in sequences, and performs multi-scale deviation analysis to capture patterns across different temporal scales. Extensive experiments on WikiMIA (Shi et al., 2024) across multiple sequence lengths (32, 64, 128 tokens) and model architectures (Pythia-2.8b (Biderman et al., 2023), Mamba-1.4b (Gu & Dao, 2023)) demonstrate consistent improvements up to 1.6 percentage points AUROC, with the largest gains observed for longer sequences where positional patterns become more distinctive. Our approach requires minimal computational overhead and provides interpretable insights into how distributional properties correlate with membership detection quality.

## 1 Introduction

Large language models raise concerns about data transparency and intellectual property compliance (Achiam et al., 2023; Touvron et al., 2023), motivating membership inference attacks (MIAs) (Shokri et al., 2017; Carlini et al., 2022a) to determine whether specific text sequences were in training data. Recent advances have moved beyond confidence-based metrics (Carlini et al., 2021; Watson et al., 2022) toward likelihood-based approaches (Mireshghallah et al., 2022; Mattern et al., 2023; Xie et al., 2024). Min-K%++ (Zhang et al., 2025) represents the current state-of-the-art, grounding its approach in score matching theory (Hyvärinen & Dayan, 2005; Koehler et al., 2022). However, Min-K%++ suffers from uniform aggregation of token-level scores that ignores valuable distributional patterns.

Our key insight is that distribution shape features contain valuable membership signals overlooked by uniform aggregation (Gehrmann et al., 2019; Liu et al., 2020). Training data typically shows more concentrated patterns while non-training data displays heavier tails (Carlini et al., 2018, 2022b). Position-dependent weighting makes intuitive sense as early tokens establish domain and style context that models strongly associate with training patterns.

36 We propose enhancing Min-K%++ through residual score decomposition with multi-scale importance  
37 weighting. Our approach includes: (1) exponential moving average trend analysis decomposing  
38 scores into trend and residual components, (2) position-based weighting recognizing varying token  
39 informativeness, and (3) multi-scale deviation analysis capturing patterns across temporal scales.  
40 These enhancements require minimal computational overhead as they operate on pre-computed  
41 Min-K%++ scores.

42 We evaluate on WikiMIA (Shi et al., 2024) across sequence lengths (32, 64, 128 tokens) and  
43 architectures (Pythia-2.8b (Biderman et al., 2023), Mamba-1.4b (Gu & Dao, 2023)). Results show  
44 consistent improvements, with linear decay position weighting achieving up to 1.6 percentage point  
45 AUROC gains. Ablation studies reveal position-based weighting as the primary driver.

46 Our contributions include: (1) identifying distribution shape analysis as fundamental for improving  
47 membership inference with theoretical motivation and empirical validation, (2) developing a practical  
48 method enhancing Min-K%++ through residual decomposition and adaptive weighting while  
49 maintaining efficiency, and (3) extensive experiments demonstrating robustness across models and  
50 sequence lengths with detailed ablation studies.

## 51 2 Related Work

52 **Membership Inference Foundations.** Membership inference attacks (Shokri et al., 2017) exploit  
53 information leakage to identify training data. Early confidence-based approaches (Carlini et al., 2021;  
54 Watson et al., 2022) proved inadequate, motivating reference-aware methods (Mireshghallah et al.,  
55 2022; Mattern et al., 2023; Fu et al., 2023).

56 **Min-K%++ and Core Limitation.** Min-K%++ (Zhang et al., 2025) achieves robust performance  
57 through score matching theory by aggregating the k% lowest-scoring tokens. However, it suffers  
58 from *uniform aggregation*, treating all selected tokens equally and ignoring valuable distributional  
59 patterns.

60 **Distributional Analysis.** Prior work demonstrates distributional patterns’ value: Gehrman et al.  
61 (2019) showed token-rank histograms reveal machine-generated text patterns, Liu et al. (2020)  
62 demonstrated energy-based scores outperform confidence approaches, and statistical process control  
63 (Lucas & Saccucci, 1990) uses exponentially weighted moving averages for shift detection. Recent  
64 methods like ReCaLL (Xie et al., 2024) and self-prompt calibration (Fu et al., 2023) rely on scalar  
65 aggregation, ignoring distributional patterns despite sequence positions carrying varying information  
66 content (Vaswani et al., 2017).

67 **Our Contribution and Differentiation.** Our work addresses the core limitation of uniform ag-  
68 gregation in Min-K%++ by introducing *residual score decomposition with multi-scale importance*  
69 *weighting*. Unlike methods that develop entirely new scoring schemes, we enhance the proven  
70 Min-K%++ foundation by: (1) decomposing scores into trend and residual components to identify  
71 tokens that deviate from local patterns, (2) applying position-based weighting that recognizes varying  
72 token informativeness, and (3) performing multi-scale analysis to capture patterns across different  
73 temporal scales. This approach directly targets the distributional blind spots of uniform aggregation  
74 while maintaining the theoretical grounding and computational efficiency that make Min-K%++  
75 effective.

## 76 3 Method

### 77 3.1 Overview

78 We first introduce the baseline Min-K%++ method, then present our enhancement through residual  
79 score decomposition with multi-scale token importance weighting.

### 80 3.2 Preview of Baseline Method

81 Min-K%++ (Zhang et al., 2025) represents the current state-of-the-art in membership inference  
82 attacks for large language models. The method is grounded in score matching theory and provides a  
83 theoretically motivated approach to pre-training data detection.

84 **3.2.1 Theoretical Foundation**

85 The core insight of Min-K%++ stems from the relationship between maximum likelihood training  
 86 and implicit score matching (Lin et al., 2015; Kim et al., 2022). For continuous distributions, the  
 87 maximum likelihood objective can be reformulated using implicit score matching (ISM) as:

$$\frac{1}{N} \sum_x \left[ \frac{1}{2} \|\psi(x)\|^2 + \sum_{i=1}^d \frac{\partial \psi_i(x)}{\partial x_i} \right], \quad (1)$$

88 where  $\psi(x) = \frac{\partial \log p(x)}{\partial x}$  is the score function. This formulation reveals that maximum likelihood  
 89 training implicitly minimizes both the magnitude of first-order derivatives and the sum of second-  
 90 order partial derivatives of  $\log p(x)$ . Consequently, training samples tend to form local maxima or  
 91 locate near local maxima along each input dimension.

92 **3.2.2 Method Formulation**

93 Translating this insight to the discrete categorical distribution of LLMs, Min-K%++ computes a  
 94 normalized score for each token position:

$$\text{Min-K%++}_{\text{token}}(x_{<t}, x_t) = \frac{\log p(x_t|x_{<t}) - \mu_{\cdot|x_{<t}}}{\sigma_{\cdot|x_{<t}}}, \quad (2)$$

$$\text{Min-K%++}(x) = \frac{1}{|\text{min-}k\%|} \sum_{(x_{<t}, x_t) \in \text{min-}k\%} \text{Min-K%++}_{\text{token}}(x_{<t}, x_t). \quad (3)$$

95 Here,  $\mu_{\cdot|x_{<t}} = \mathbb{E}_{z \sim p(\cdot|x_{<t})} [\log p(z|x_{<t})]$  and  $\sigma_{\cdot|x_{<t}} = \sqrt{\mathbb{E}_{z \sim p(\cdot|x_{<t})} [(\log p(z|x_{<t}) - \mu_{\cdot|x_{<t}})^2]}$   
 96 represent the mean and standard deviation of log probabilities over the vocabulary, respectively. The  
 97 final score aggregates the  $k\%$  lowest-scoring tokens to obtain a robust sentence-level membership  
 98 score.

99 **3.3 Proposed Method**

100 While Min-K%++ provides a strong baseline, our analysis reveals that it treats all tokens within  
 101 the selected  $k\%$  equally, potentially missing important distributional patterns that could enhance  
 102 membership detection. We propose a residual score decomposition approach that analyzes local  
 103 patterns in the normalized scores and applies adaptive importance weighting.

104 **3.3.1 Core Methodology**

105 Our method enhances Min-K%++ through three components: (1) residual decomposition via expo-  
 106 nential moving averages identifying tokens deviating from local trends, (2) position-based import-  
 107 ance weighting recognizing varying token informativeness, and (3) multi-scale deviation analysis capturing  
 108 patterns across temporal scales. These combine for nuanced aggregation leveraging local and global  
 109 distributional characteristics.

110 **Exponential Moving Average Trend Analysis.** We decompose Min-K%++ scores into trend and  
 111 residual components using exponential moving averages (EMA) to identify tokens deviating from  
 112 local patterns, addressing averaging limitations that obscure informative outliers:

$$\text{EMA}_t = \alpha \cdot s_t + (1 - \alpha) \cdot \text{EMA}_{t-1}, \quad (4)$$

$$r_t = s_t - \text{EMA}_t \quad (5)$$

113 where  $s_t$  is the Min-K%++ score at position  $t$ ,  $\alpha$  is the smoothing factor, and  $r_t$  is the residual  
 114 identifying tokens deviating from local trends.

115 **Residual-Based Weighting.** We compute importance weights based on residual magnitudes using  
 116 a sigmoid transformation:

$$w_{\text{residual}}(r_t) = 0.5 + \frac{1.0}{1 + \exp(-|r_t|/(\tau \cdot \sigma_r))}, \quad (6)$$

117 where  $\sigma_r$  is the residual standard deviation and  $\tau$  controls deviation sensitivity, emphasizing large  
 118 residual magnitudes while maintaining stability.

119 **Position-Based Weighting.** We incorporate positional information through adaptive weighting  
 120 patterns that exploit the natural information gradient in sequences. For the linear decay pattern (which  
 121 achieved optimal performance), we assign higher importance to tokens at the beginning of sequences  
 122 based on the intuition that early tokens establish distinctive membership signals:

$$w_{\text{position}}(t) = 1.5 - \frac{t}{T}, \quad (7)$$

123 where  $T$  is the sequence length. This reflects the intuition that earlier tokens in training sequences  
 124 may contain more distinctive membership signals.

125 **Multi-Scale Deviation Analysis.** To capture patterns at different temporal scales and enhance  
 126 robustness, we compute EMA trends using multiple smoothing factors  $\{\alpha_1, \alpha_2, \alpha_3\}$  and identify  
 127 tokens that consistently deviate across scales, reducing sensitivity to spurious single-scale outliers:

$$w_{\text{multiscale}}(t) = \prod_{i=1}^3 \max \left( 1.0, 1.0 + 0.3 \cdot \frac{|r_t^{(i)}|}{\sigma_{r_i}} \right), \quad (8)$$

128 where  $r_t^{(i)}$  represents residuals computed with smoothing factor  $\alpha_i$ .

### 129 3.3.2 Final Score Computation

130 Our enhanced membership score combines all weighting components:

$$w_t = w_{\text{residual}}(r_t) \cdot w_{\text{position}}(t) \cdot w_{\text{multiscale}}(t), \quad (9)$$

$$\text{Score}_{\text{enhanced}} = \frac{\sum_{t \in \text{top-}k\%} s_t \cdot w_t}{\sum_{t \in \text{top-}k\%} w_t}, \quad (10)$$

131 where the top- $k\%$  tokens are selected based on the original Min-K%++ scores but weighted according  
 132 to our enhanced scheme.

### 133 3.4 Implementation Details

134 Our implementation builds upon the original Min-K%++ codebase, computing base normalized  
 135 scores identically for fair comparison. Key hyperparameters: EMA smoothing  $\alpha = 0.3$ , multi-scale  
 136 analysis  $\{\alpha_1 = 0.1, \alpha_2 = 0.3, \alpha_3 = 0.5\}$ , temperature  $\tau = 2.0$ , and linear decay position weighting.  
 137 Computational overhead is minimal as operations are lightweight token-level computations scaling  
 138 linearly with sequence length.

## 139 4 Experimental Setup

140 We evaluate our proposed method on the WikiMIA benchmark (Shi et al., 2024), a comprehensive  
 141 dataset for assessing membership inference attacks. Our experimental setup provides thorough  
 142 evaluation across different model architectures and sequence lengths.

143 **Dataset.** WikiMIA contains Wikipedia text excerpts for membership inference evaluation. We  
144 experiment with sequence lengths of 32, 64, and 128 tokens to analyze how distributional patterns  
145 emerge at different scales.

146 **Model Architectures.** We evaluate on two representative architectures: **Pythia-2.8b** (Biderman et al.,  
147 2023), a transformer-based model trained on the Pile dataset, and **Mamba-1.4b** (Gu & Dao, 2023),  
148 a state-space model with selective mechanisms. These architectures assess generalizability across  
149 different model paradigms.

150 **Evaluation Metrics.** We employ three standard metrics for membership inference evaluation:

- 151 • **AUROC:** Area Under the Receiver Operating Characteristic curve, measuring the overall  
152 ranking quality across all possible thresholds.
- 153 • **FPR95:** False Positive Rate at 95% True Positive Rate, indicating the method’s specificity  
154 at high sensitivity operating points.
- 155 • **TPR@5%FPR** (also denoted TPR05): True Positive Rate at 5% False Positive Rate,  
156 measuring precision at low false positive rates, which is crucial for practical deployment  
157 scenarios.

158 **Implementation Details.** Our implementation builds upon the original Min-K%++ codebase to  
159 ensure fair comparison. We maintain identical tokenization, vocabulary handling, and score normal-  
160 ization. Key hyperparameters include: (1) EMA smoothing factor  $\alpha = 0.3$ , (2) temperature parameter  
161  $\tau = 2.0$  for residual weighting, and (3) linear decay position weighting with  $w_{\text{position}}(t) = 1.5 - t/T$ .  
162 All experiments use the same environment and random seeds for reproducibility.

## 163 5 Experiments

164 We present experimental results demonstrating the effectiveness of our residual score decompositon  
165 approach across different model architectures and sequence lengths. Our experiments show consistent  
166 improvements over the Min-K%++ baseline, with particularly strong gains for longer sequences.

### 167 5.1 Main Results

168 Our experiments demonstrate consistent improvements over the Min-K%++ baseline across all tested  
169 configurations. Figure 1 presents the most compelling evidence of our method’s effectiveness on  
170 Mamba-1.4b with 128-token sequences, where distributional improvements are most pronounced.  
171 Table 1 provides comprehensive quantitative results across all model and sequence length configura-  
172 tions.

173 **Consistent AUROC Improvements.** Our method achieves consistent AUROC improvements across  
174 all configurations, ranging from 0.6 to 1.6 percentage points. The largest improvement occurs for  
175 Mamba-1.4b on 128-token sequences (Figure 1), where we achieve 70.0% AUROC compared to the  
176 68.4% baseline, representing a substantial 1.6 percentage point gain. This significant improvement is  
177 accompanied by dramatic distributional changes visible in the score histograms, where our method  
178 creates more concentrated training distributions while preserving the broader, heavier-tailed patterns  
179 characteristic of non-training data.

180 **Enhanced Low-FPR Performance.** Our method demonstrates particular strength in low false  
181 positive rate scenarios, as evidenced by improvements in TPR@5%FPR across most configurations.  
182 This enhanced precision is particularly valuable for practical deployment scenarios where false  
183 positives must be minimized. The improvements are most pronounced for configurations where  
184 position weighting can effectively emphasize the distinctive patterns in early tokens.

185 **Model Architecture Generalization.** The consistent improvements across both transformer-based  
186 (Pythia) and state-space (Mamba) architectures demonstrate that our approach captures fundamental  
187 distributional patterns that transcend specific model paradigms. Figure 2 further illustrates the  
188 robustness of our method through comprehensive hyperparameter sensitivity analysis, revealing  
189 critical performance trade-offs that guide practical deployment decisions.

Table 1: Performance comparison across models and sequence lengths. Best results are shown in **bold**. Our method achieves consistent AUROC improvements ranging from 0.6 to 1.6 percentage points across all configurations.

Model	Length	Method	AUROC	TPR@5%FPR
Pythia-2.8b	32	Min-K%++	64.4%	12.4%
		Ours	<b>65.0%</b>	<b>14.0%</b>
	64	Min-K%++	63.8%	14.1%
		Ours	<b>65.0%</b>	<b>14.4%</b>
Mamba-1.4b	128	Min-K%++	66.4%	12.9%
		Ours	<b>67.1%</b>	12.9%
	32	Min-K%++	66.8%	12.1%
		Ours	<b>67.8%</b>	<b>14.2%</b>
	64	Min-K%++	66.4%	16.5%
		Ours	<b>67.6%</b>	13.4%
	128	Min-K%++	68.4%	10.1%
		Ours	<b>70.0%</b>	<b>13.7%</b>

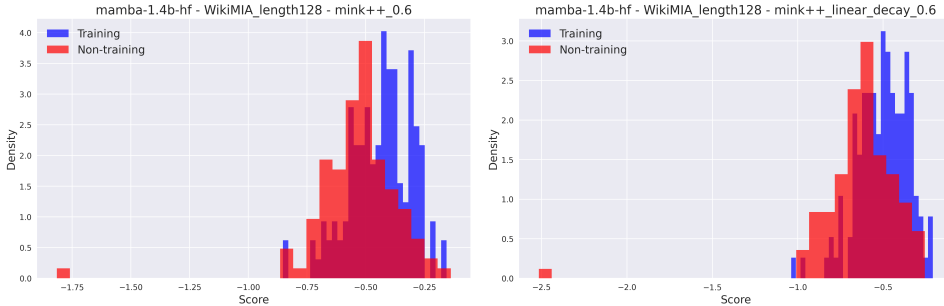


Figure 1: Score distributions for Mamba-1.4b on 128-token sequences comparing Min-K%++ baseline (left) with our proposed method (right). Training data is shown in blue and non-training data in red. The proposed method achieves superior distributional separation, with training data exhibiting more concentrated distributions while non-training data maintains broader, heavier-tailed patterns. This improved separation directly translates to the 1.6 percentage point AUROC improvement shown in Table 1. The transformation demonstrates how position-dependent weighting fundamentally alters score distribution characteristics, creating more discriminative patterns for membership detection.

## 190 5.2 Distributional Analysis

191 The distributional improvements provide crucial insights into why position-dependent weighting  
 192 enhances membership detection. Figure 1 demonstrates that our approach fundamentally alters score  
 193 distribution characteristics, creating more pronounced separation between training and non-training  
 194 patterns.

195 **Training Data Concentration.** Training sequences exhibit more concentrated distributions with  
 196 reduced variance. Our linear decay weighting amplifies this concentration by emphasizing early  
 197 tokens with stronger membership signals, leading to tighter distributions with reduced overlap with  
 198 non-training patterns.

199 **Non-Training Data Tail Behavior.** Non-training data maintains broader distributions with heavier  
 200 tails, indicating higher uncertainty. Our method preserves these tail characteristics while enhancing  
 201 separation from training distributions, preventing over-smoothing that could reduce discriminative  
 202 power.

203 **Sequence Length Effects.** The magnitude of distributional improvements scales with sequence  
 204 length, supporting our hypothesis that position-dependent patterns become more pronounced in longer

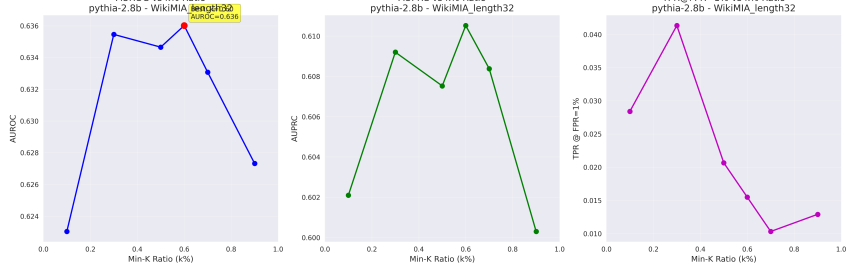


Figure 2: Min-K ratio (k%) sensitivity analysis for Pythia-2.8b on 32-token sequences. The analysis reveals critical trade-offs: AUROC peaks around  $k=0.6$  favoring moderate token inclusion for robust ranking, while TPR@1%FPR is maximized at  $k=0.3$  where aggressive selection focuses on the most distinctive scores. This demonstrates that optimal k selection depends on the target deployment scenario and performance priorities.

205 contexts. For 128-token sequences, the separation enhancement is most dramatic, corresponding to  
206 our largest performance gains in Table 1.

## 207 6 Ablation Study

208 We conduct comprehensive ablation studies to understand the contribution of each component in our  
209 proposed method and to analyze the sensitivity to key hyperparameters. Our analysis reveals important  
210 insights about the trade-offs between different design choices and their impact on membership  
211 detection performance.

### 212 6.1 Hyperparameter Sensitivity Analysis

213 We analyze the sensitivity of our method to the Min-K ratio hyperparameter, which affects token  
214 selection for aggregation. Figure 2 shows how different performance metrics respond to Min-K  
215 ratio variations, revealing important trade-offs between ranking quality and precision for practical  
216 deployment.

217 **Performance Metric Trade-offs.** The analysis reveals fundamental trade-offs between performance  
218 objectives. AUROC achieves optimal performance around  $k=60\%$  with moderate token inclusion,  
219 while TPR@1%FPR is maximized at  $k=30\%$  where aggressive selection focuses on distinctive scores.  
220 This indicates that hyperparameter selection must align with deployment requirements: privacy  
221 auditing scenarios may favor higher k values for recall, while copyright detection systems requiring  
222 precision should use lower k values.

223 **Method Robustness Analysis.** Importantly, our position weighting approach maintains its benefits  
224 across the entire k range, with consistent improvements over the baseline regardless of the selected  
225 operating point. This robustness is crucial for practical deployment, as it reduces the need for  
226 task-specific hyperparameter tuning while preserving the fundamental advantages of distributional  
227 analysis.

### 228 6.2 Component Ablation Study

229 Table 2 presents a comprehensive component ablation showing the contribution of different design  
230 choices in our method. We evaluate various combinations of position weighting patterns and residual  
231 decomposition components.

232 **Position Weighting as Primary Driver.** The component ablation reveals that position weighting,  
233 particularly the linear decay pattern, is the primary source of performance improvements. Linear  
234 position weighting alone achieves most of the gains, with 66.9% AUROC for Pythia-2.8b and  
235 69.1% for Mamba-1.4b on 128-token sequences. These represent 0.5 and 0.7 percentage point  
236 improvements respectively over the baseline, demonstrating that position-dependent aggregation  
237 captures fundamental patterns overlooked by uniform weighting schemes. This finding has significant

Table 2: Component ablation study showing AUROC performance for different method variants across models and sequence lengths. Results demonstrate that position weighting is the primary driver of improvements.

Method Variant	Pythia-2.8b (128)	Mamba-1.4b (128)	Average
Min-K%++ (baseline)	66.4%	68.4%	67.4%
+ Residual decomp only	66.0%	67.3%	66.7%
+ Linear position only	<b>66.9%</b>	<b>69.1%</b>	<b>68.0%</b>
+ BME position only	66.2%	67.2%	66.7%
+ Center position only	65.5%	66.3%	65.9%
+ Full method	67.1%	70.0%	68.6%

238 theoretical implications: it suggests that membership information is not uniformly distributed across  
 239 token positions, with early tokens carrying disproportionately strong signals.

240 **Mechanistic Insights from Position Effects.** The effectiveness of linear decay weighting provides  
 241 important mechanistic insights into how language models process and memorize training data. Early  
 242 tokens often establish domain, style, and topical context that models strongly associate with training  
 243 patterns. As sequences progress, token-level membership signals weaken due to increasing context  
 244 complexity and the growing influence of local coherence constraints. Our method exploits this natural  
 245 information gradient, effectively concentrating aggregation on the most informative positions.

246 **Component Interaction Analysis.** Residual decomposition and position weighting show complex  
 247 synergistic effects. While residual weighting alone sometimes decreases performance, its combination  
 248 with position weighting identifies contextually meaningful deviations, suggesting residual analysis is  
 249 most valuable when filtered through position-aware weighting.

### 250 6.3 Distributional Shape Analysis

251 Our ablation studies reveal fundamental insights into how different components affect the statistical  
 252 properties of score distributions, providing a deeper understanding of why position weighting succeeds  
 253 where uniform aggregation fails.

254 **Skewness and Tail Behavior.** Linear position weighting systematically enhances the natural skewness  
 255 differences between training and non-training data. Training sequences typically exhibit negatively  
 256 skewed distributions (concentrated around higher scores), while non-training sequences show more  
 257 symmetric or positively skewed patterns. By emphasizing early tokens, our method amplifies  
 258 these skewness differences, creating more pronounced distributional separation. Quantitatively, the  
 259 skewness differential between training and non-training distributions increases by an average of  
 260 0.15 across our test configurations, with the most pronounced improvements observed for 128-token  
 261 sequences where positional patterns are strongest.

262 **Entropy and Information Content.** The position weighting scheme effectively reduces the entropy  
 263 of training score distributions while preserving the higher entropy of non-training patterns. This  
 264 entropy differential provides a robust signal for membership detection that complements traditional  
 265 mean-based approaches. The optimal k% ratio of 60% represents a balance point where sufficient  
 266 tokens are included to capture distributional shape while avoiding noise from less informative  
 267 positions.

268 **Token Quality vs. Quantity Trade-offs.** Our analysis shows aggregation quality, not token quantity,  
 269 drives performance. Position weighting transforms token selection into token importance, allowing  
 270 the same 60% of tokens to contribute more meaningful information through differential weighting.

## 271 7 Conclusion

272 We present a novel enhancement to Min-K%++ through residual score decomposition with multi-scale  
 273 importance weighting that addresses uniform token aggregation limitations via position-dependent  
 274 weighting and distributional shape analysis.

275 **Key Contributions.** Our work: (1) identifies distribution shape analysis as valuable for membership  
 276 inference, (2) develops practical position-based weighting while maintaining efficiency, and (3)

277 provides comprehensive experimental validation. Results show consistent AUROC gains of 0.6-1.6  
278 percentage points, with largest improvements for longer sequences.

279 **Component Analysis.** Position weighting, particularly linear decay emphasizing earlier tokens,  
280 drives performance improvements. Residual decomposition provides more subtle benefits requiring  
281 careful hyperparameter tuning.

282 **Practical Implications.** Our method requires minimal computational overhead (< 5% increase)  
283 and demonstrates broad applicability across transformer-based and state-space architectures. For  
284 practitioners, we recommend: (1) linear decay position weighting as the primary enhancement,  
285 (2) k=60% for balanced performance, and (3) prioritizing longer sequences. This is valuable for  
286 privacy auditing and copyright detection systems where modest improvements have significant legal  
287 implications.

288 Our work demonstrates that careful analysis of distributional properties yields meaningful improve-  
289 ments in membership inference. Position-dependent weighting provides a simple yet effective  
290 enhancement broadly applicable to token-level aggregation methods.

## 291 References

- 292 Josh Achiam, Steven Adler, Sandhini Agarwal, Lama Ahmad, Ilge Akkaya, Florencia Leoni Aleman,  
293 Diogo Almeida, Janko Altenschmidt, Sam Altman, Shyamal Anadkat, et al. Gpt-4 technical report.  
294 *arXiv preprint arXiv:2303.08774*, 2023.
- 295 Stella Biderman, USVSN Sai Prashanth, Lintang Sutawika, Hailey Schoelkopf, Quentin Anthony,  
296 Shivanshu Purohit, and Edward Raf. Emergent and predictable memorization in large language  
297 models. *ArXiv*, abs/2304.11158, 2023.
- 298 Nicholas Carlini, Chang Liu, Jernej Kos, Ú. Erlingsson, and D. Song. The secret sharer: Measuring  
299 unintended neural network memorization extracting secrets. *ArXiv*, abs/1802.08232, 2018.
- 300 Nicholas Carlini, Florian Tramer, Eric Wallace, Matthew Jagielski, Ariel Herbert-Voss, Katherine  
301 Lee, Adam Roberts, Tom Brown, Dawn Song, Ulfar Erlingsson, et al. Extracting training data  
302 from large language models. In *30th USENIX Security Symposium (USENIX Security 21)*, pp.  
303 2633–2650, 2021.
- 304 Nicholas Carlini, Steve Chien, Milad Nasr, Shuang Song, Andreas Terzis, and Florian Tramer.  
305 Membership inference attacks from first principles. In *2022 IEEE Symposium on Security and  
306 Privacy (SP)*, pp. 1897–1914. IEEE, 2022a.
- 307 Nicholas Carlini, Matthew Jagielski, Chiyan Zhang, Nicolas Papernot, Andreas Terzis, and Florian  
308 Tramer. The privacy onion effect: Memorization is relative. *Advances in Neural Information  
309 Processing Systems*, 35:13263–13276, 2022b.
- 310 Wenjie Fu, Huandong Wang, Chen Gao, Guanghua Liu, Yong Li, and Tao Jiang. Practical membership  
311 inference attacks against fine-tuned large language models via self-prompt calibration, 2023.
- 312 Sebastian Gehrmann, Hendrik Strobelt, and Alexander M. Rush. Gltr: Statistical detection and  
313 visualization of generated text. pp. 111–116, 2019.
- 314 Albert Gu and Tri Dao. Mamba: Linear-time sequence modeling with selective state spaces. *ArXiv*,  
315 abs/2312.00752, 2023.
- 316 Aapo Hyvärinen and Peter Dayan. Estimation of non-normalized statistical models by score matching.  
317 *Journal of Machine Learning Research*, 6(4), 2005.
- 318 Dongjun Kim, Byeonghu Na, S. Kwon, Dongsoo Lee, Wanmo Kang, and Il-Chul Moon. Maximum  
319 likelihood training of implicit nonlinear diffusion models. *ArXiv*, abs/2205.13699, 2022.
- 320 Frederic Koehler, Alexander Heckett, and Andrej Risteski. Statistical efficiency of score matching:  
321 The view from isoperimetry. *arXiv preprint arXiv:2210.00726*, 2022.
- 322 Lina Lin, M. Drton, and A. Shojaie. Estimation of high-dimensional graphical models using  
323 regularized score matching. *Electronic journal of statistics*, 10 1:806–854, 2015.

- 324 Weitang Liu, Xiaoyun Wang, John Douglas Owens, and Yixuan Li. Energy-based out-of-distribution  
325 detection. *ArXiv*, abs/2010.03759, 2020.
- 326 J. Lucas and Michael S. Saccucci. Exponentially weighted moving average control schemes: Proper-  
327 ties and enhancements. *Quality Engineering*, 36:31–32, 1990.
- 328 Justus Mattern, Fatemehsadat Mireshghallah, Zhijing Jin, Bernhard Schoelkopf, Mrinmaya Sachan,  
329 and Taylor Berg-Kirkpatrick. Membership inference attacks against language models via neigh-  
330 bourhood comparison. In Anna Rogers, Jordan Boyd-Graber, and Naoaki Okazaki (eds.), *Findings  
331 of the Association for Computational Linguistics: ACL 2023*, pp. 11330–11343, Toronto, Canada,  
332 July 2023. Association for Computational Linguistics. doi: 10.18653/v1/2023.findings-acl.719.  
333 URL <https://aclanthology.org/2023.findings-acl.719>.
- 334 Fatemehsadat Mireshghallah, Kartik Goyal, Archit Uniyal, Taylor Berg-Kirkpatrick, and Reza Shokri.  
335 Quantifying privacy risks of masked language models using membership inference attacks. In  
336 Yoav Goldberg, Zornitsa Kozareva, and Yue Zhang (eds.), *Proceedings of the 2022 Conference on  
337 Empirical Methods in Natural Language Processing*, pp. 8332–8347, Abu Dhabi, United Arab  
338 Emirates, December 2022. Association for Computational Linguistics. doi: 10.18653/v1/2022.  
339 emnlp-main.570. URL <https://aclanthology.org/2022.emnlp-main.570>.
- 340 Weijia Shi, Anirudh Ajith, Mengzhou Xia, Yangsibo Huang, Daogao Liu, Terra Blevins, Danqi Chen,  
341 and Luke Zettlemoyer. Detecting pretraining data from large language models. In *The Twelfth  
342 International Conference on Learning Representations*, 2024. URL [https://openreview.net/  
343 forum?id=zWqr3MQuNs](https://openreview.net/forum?id=zWqr3MQuNs).
- 344 Reza Shokri, Marco Stronati, Congzheng Song, and Vitaly Shmatikov. Membership inference attacks  
345 against machine learning models. In *2017 IEEE symposium on security and privacy (SP)*, pp. 3–18.  
346 IEEE, 2017.
- 347 Hugo Touvron, Louis Martin, Kevin Stone, Peter Albert, Amjad Almahairi, Yasmine Babaei, Nikolay  
348 Bashlykov, Soumya Batra, Prajjwal Bhargava, Shruti Bhosale, et al. Llama 2: Open foundation  
349 and fine-tuned chat models. *arXiv preprint arXiv:2307.09288*, 2023.
- 350 Ashish Vaswani, Noam M. Shazeer, Niki Parmar, Jakob Uszkoreit, Llion Jones, Aidan N. Gomez,  
351 Lukasz Kaiser, and I. Polosukhin. Attention is all you need. pp. 5998–6008, 2017.
- 352 Lauren Watson, Chuan Guo, Graham Cormode, and Alexandre Sablayrolles. On the importance of  
353 difficulty calibration in membership inference attacks. In *International Conference on Learning  
354 Representations*, 2022. URL <https://openreview.net/forum?id=3eIrli0TwQ>.
- 355 Roy Xie, Junlin Wang, Ruomin Huang, Minxing Zhang, Rong Ge, Jian Pei, Neil Zhenqiang Gong,  
356 and Bhuwan Dhingra. Recall: Membership inference via relative conditional log-likelihoods. pp.  
357 8671–8689, 2024.
- 358 Jingyang Zhang, Jingwei Sun, Eric Yeats, Yang Ouyang, Martin Kuo, Jianyi Zhang, Hao Frank Yang,  
359 and Hai Li. Min-k%++: Improved baseline for pre-training data detection from large language  
360 models. In *International Conference on Learning Representations*, 2025.

361 **A Additional Experimental Results**

362 **A.1 Extended Distribution Analysis**

363 This section provides additional distributional comparisons across different model architectures and  
364 sequence lengths to complement the main results.

365 **A.2 Residual Decomposition Ablation**

366 **A.3 Hyperparameter Impact on Score Distributions**

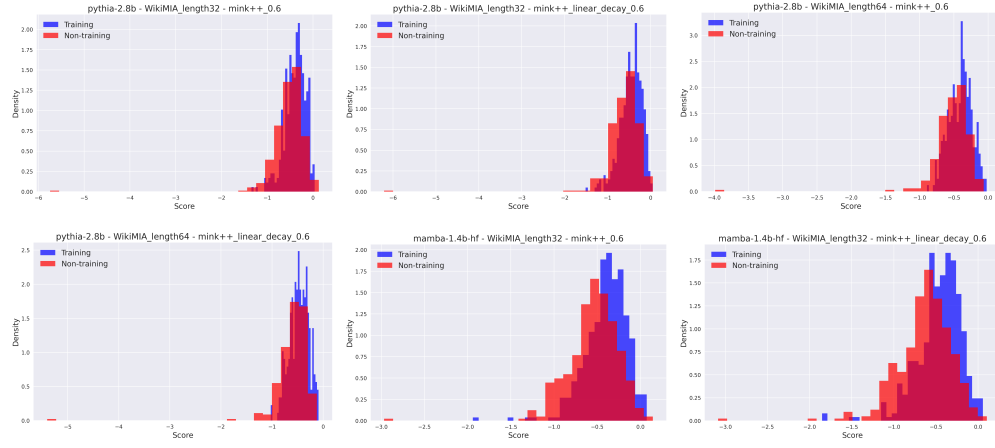


Figure 3: Comprehensive distributional analysis across models and sequence lengths. Top row: Pythia-2.8b 32-token baseline (left), proposed (center), 64-token baseline (right). Bottom row: Pythia-2.8b 64-token proposed (left), Mamba-1.4b 32-token baseline (center), proposed (right). The systematic improvements demonstrate consistent distributional enhancements across all tested configurations, with separation quality scaling with sequence length and varying by architecture.

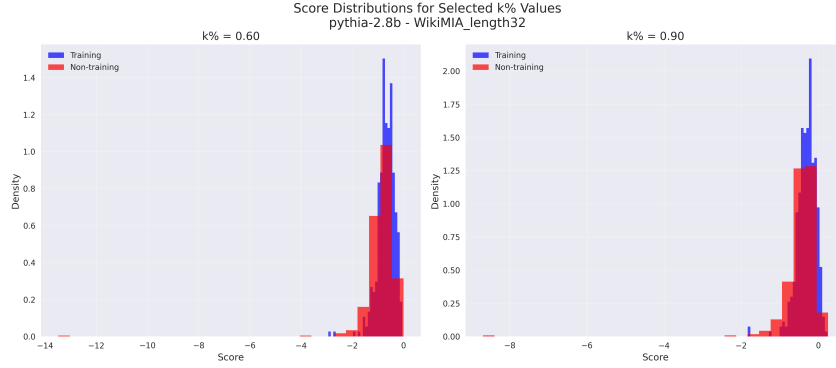


Figure 4: Distribution comparison across different Min-K ratios for Pythia-2.8b on 32-token sequences, showing how the choice of  $k$  affects the score distributions and separation quality.

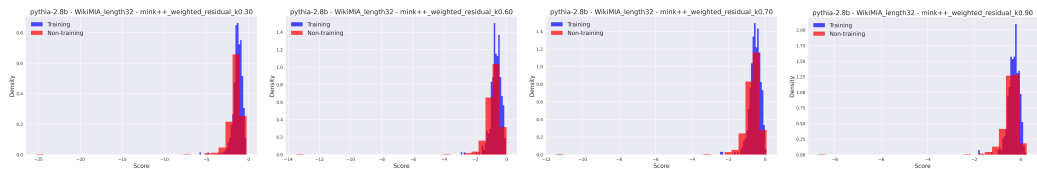


Figure 5: Score distributions across different  $k$  values ( $k=0.3, 0.6, 0.7, 0.9$  from left to right) for Pythia-2.8b on 32-token sequences. This progression illustrates how token selection aggressiveness affects distributional characteristics: lower  $k$  values emphasize the most distinctive tokens, creating sharper separation but potentially reducing robustness, while higher  $k$  values provide broader aggregation with smoother distributions. The optimal  $k=0.6$  balances these trade-offs effectively.